Low-Temperature Synthesis of Amorphous Carbon Nanocoils via Acetylene Coupling on Copper Nanocrystal Surfaces at 468 K: A Reaction Mechanism Analysis

Yong Qin and Xin Jiang*

Institut für Werkstofftechnik, Universität Siegen, Paul-Bonartz-Strasse 9, 57068 Siegen, Germany

Zuolin Cui

Key Laboratory of Nanomaterials, Qingdao University of Science and Technology, Qingdao 266042, P. R. China

Received: August 8, 2005; In Final Form: September 19, 2005

A new type of amorphous helical carbon nanofibers has been synthesized using copper nanocatalysts and an acetylene gas source at atmospheric pressure. The nanofibers are grown at 468 K, which is the lowest temperature by ordinary metal-catalyzed thermal chemical vapor deposition of hydrocarbon, and exhibit a symmetric growth mode in the form of twin helices. IR, XRD, Raman, and C/H molar ratio analyses reveal a polymer-like structure with a weak *trans*-polyacetylene feature. The nanofibers are a mixture of solid polymers and a small amount of carbon. A reaction mechanism has been proposed on the basis of the previous studies of acetylene adsorption, desorption properties, and surface reactions on copper (111), (110), and (001) planes under ultrahigh-vacuum (UHV) conditions as well as the results obtained in our study. The reaction mechanism of acetylene on copper single-crystal surfaces under UHV conditions indeed reflects the reaction mechanism under practical catalytic conditions at atmospheric pressure. The nanofibers grow mainly via acetylene coupling to solid polymers on copper nanocrystal surfaces. Acetylene also couples to yield small amounts of liquid oligomers and gaseous products, and undergoes slight carbon deposition during the fiber growth.

1. Introduction

Acetylene is an important chemical reagent. It is well-known that polymerization of acetylene produces polyacetylene by homogeneous catalysis at low temperature, usually below room temperature.[1,2] Shirakawa et al. synthesized polyacetylene at a higher temperature of 423 K.[3] Carbon nanostructures, mainly carbon nanofibers and nanotubes, can be synthesized by metal powder catalyzed chemical vapor deposition with acetylene as a carbon source at high temperature.[4−7] Metals such as nickel, cobalt, and iron (or their alloys) are usually used. It is proposed that carbon produced by the thermal decomposition of acetylene can dissolve in and diffuse through metal particles, and precipitate to form carbon nanostructures.[8−11] However, carbon cannot dissolve in metal copper, even if there are reports that copper alloy such as Cu−Ni can catalyze the carbon deposition of hydrocarbon; consequently, pure metal copper is inactive for the growth of carbon nanostructures.[12−14]

On the other hand, the study of the interaction of hydrocarbon such as acetylene with metal low-index single-crystal surfaces under UHV conditions has been an extraordinarily active area for a long time.[15−22] These studies can contribute to a fundamental understanding of catalytically important surface processes, unravel fundamental mechanisms in heterogeneous catalysis, and identify important surface intermediates in practical reactions. The adsorption and surface reactions of acetylene on copper low-index surfaces (110, 001, and 111) under UHV conditions has been widely investigated by both theoretical and experimental methods.[23−35] Relatively early, Outka et al. observed the surface reaction of acetylene on copper surfaces.[23] Acetylene was largely nondissociatively adsorbed on Cu(110) with acetylene desorption peaks at 280, 340, and 375 K. Ethylene formation was detected with a desorption maximum occurring at 340 K. Acetylene desorption was complete over 420 K, and approximately 11% of the carbon initially adsorbed in the acetylene remained on the surface following ethylene desorption. The carbon binding energy corresponded to the value of 284.3 eV ascribed previously to atomic carbon on Cu(110). Later, Avery found that trimerization to benzene was the main surface process of acetylene on Cu(110).[24] In particular, their work showed that Outka et al. failed to detect the major desorption product, benzene, and erroneously attributed its mass spectrometric fragments to ethylene. They also observed that after the sample was heated to 400 K the electron energy loss (EEL) spectrum reveal weak bands near 770, 870, and 3010 cm^{-1}. The 870 cm^{-1} band was attenuated after heating to 600 K. The remaining two bands survived 700 K but were attenuated after 800 K. These spectra showed that reaction-limited hydrogen evolution was associated with the destructive dehydrogenation of newly adsorbed hydrocarbon residues formed concomitantly with acetylene desorption and trimerization. Marinova et al. investigated the acetylene adsorption on the Cu(001) surface. They observed that heating to 375 K resulted in simultaneous desorption of acetylene and formation of new hydrocarbon species.[25] Later, Dvorak et al. identified the trimerization of acetylene to benzene on the Cu(001) surface.[26] The benzene formation was the major reaction. Another reaction channel was a decomposition/isomerization of acetylene leading to a strongly bound surface species. They measured the amount of acetylene that decomposed/isomerized on the surface rather than desorbed. At saturation coverage, about 5% acetylene decomposed/isomerized to an irreversibly bound hydrocarbon

* To whom correspondence should be addressed. E-mail: xin.jiang@uni-siegen.de Tel.: 49-271-7402966. Fax: 49-271-7402442.

10.1021/jp054412b CCC: $30.25
Published on Web 10/21/2005

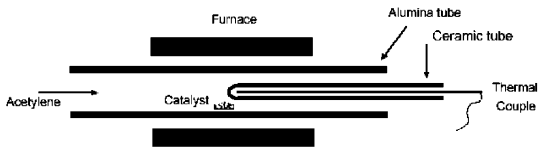

Figure 1. Schematic diagram of the synthesis apparatus.

species after performing a thermal desorption spectrum (TDS) run to 420 K. Very recently, Kyriakou et al. reported that acetylene trimerized to benzene on Cu(111).[27] However, Cu(111) also yielded ethylene, butadiene, and cyclooctatetraene. Ethylene and butadiene formation meant the possibility of C−H cleavage to produce hydrogen and carbon, although they reported no detectable carbon deposition by C 1s X-ray photoelectron spectroscopy (XPS), consistent with the relatively small amounts of C−H cleavage necessary to produce enough hydrogen to account for the small yields of ethylene and butadiene formation. They also carried out a catalytic measurement using alumina-supported copper nanoparticles at atmospheric pressure of a 10:1 hydrogen/acetylene mixture at 523 K (H_2 was used to inhibit carbon deposition). They found that these dispersed copper nanoparticles yielded the same principal reaction products as those found with Cu(111) under UHV conditions. The principal products were benzene, butadiene, and cyclooctatetraene. In addition, much smaller amounts of butene, ethylene, and C_n ($n = 10, 12, 14$) hydrocarbons were detected. They suggested that the rapid falloff of the initial activity to a lower quasi steady-state value was consistent with extensive deposition of hydrocarbonaceous species with high molecular weight.

In previous works, we reported the growth of novel helical nanofibers on copper nanoparticles using acetylene as a gas source at atmospheric pressure in the 523−673 K temperature region.[36,37] In this work, we present the acetylene reaction on copper nanocrystals at the lowest temperature of 468 K. The morphologies and structures of the obtained helical nanofibers are investigated. In particular, the reaction mechanism associated with the nanofiber formation has been discussed in detail on the basis of the available results of the interaction of acetylene with copper surfaces under UHV conditions. The nanofibers grow principally via an acetylene-coupling mechanism, not the ordinary thermal decomposition mechanism. This is the reason nanofibers are obtained using copper nanocatalysts although pure metal copper is inactive for carbon deposition.

2. Experimental Methods

In this study, copper nanoparticles are prepared by the reduction of copper sulfate with sodium borohydride. In a typical experiment, 100 mL of copper sulfate aqueous solution (0.01 M) is taken in a conical flask. Then, 100 mL of ice-cold sodium borohydride aqueous solution (0.01 M) is dropped slowly into the former solution with stirring. The obtained copper nanoparticles are filtered, washed with anhydrous ethanol, dispersed in a ceramic plate, and then transferred to the reactor. The schematic diagram of the synthesis system is shown in Figure 1. An alumina tube with a 1-cm wall thickness is used as the reactor. After the tube is evacuated to a low base pressure, acetylene is introduced to an atmospheric pressure, and the tube is heated. To determine the lowest reaction temperature, the tube is slowly heated at a rate of 1 K/min. When the temperature increases to a certain value, namely, the triggering temperature, acetylene begins to deposit on copper nanoparticles (at this point, the pressure inside the tube begins to decrease obviously). Keep the temperature constant for 10 min, then pump the residual gas, cool the reactor to room temperature, and take out the resultant nanofibers.

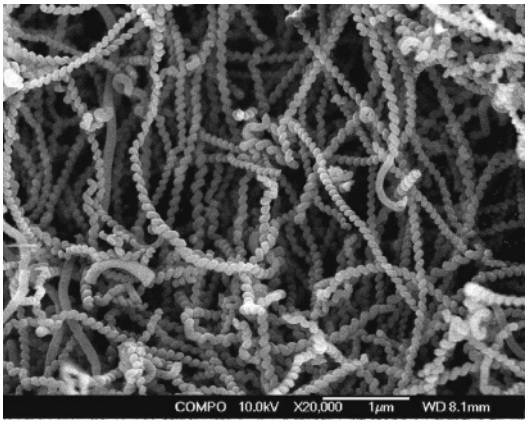

Figure 2. FE-SEM image of as-grown helical nanofibers.

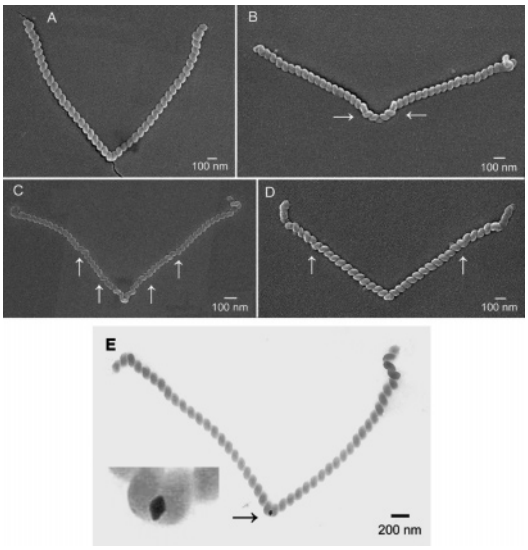

Figure 3. Twin helices with a symmetric growth mode. FE-SEM image of twin helices (A) without helical reversals and (B−D) with helical reversals indicated by arrows. (E) TEM image of twin helices grown on a single copper nanocrystal (the inset is magnified image of the copper nanocrystal indicated by arrow).

3. Results

The experimental results are that helical nanofibers can be synthesized with copper nanocatalyst at the lowest temperature of 468 K. In addition, at both ends of the reactor (here, the temperature is much lower than in the middle section), there is some liquid product, which must have been formed concomitantly with the nanofiber formation and then condensed here. Figure 2 shows a representative field emission scanning electron microscopy (FE-SEM) image of helical nanofibers. These regular nanofibers are tightly coiled in the form of a single helix. They have uniform coil diameters of about 100 nm and small coil pitches also about 100 nm. The length of these nanofibers is on the order of 1 μm. FE-SEM and transmission electron microscope (TEM) investigations reveal that these nanofibers always present a symmetric growth mode, i.e., they are always in the feature of twin helices, as shown in Figure 3. The two twin helices grown over a single copper nanocrystal have identical coil diameter, coil length, coil pitch, fiber diameter, cross-section, and cycle number. However, their helical senses or directions are absolutely different. They usually change

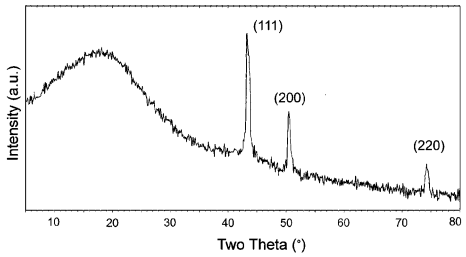

Figure 4. XRD patterns of helical nanofibers.

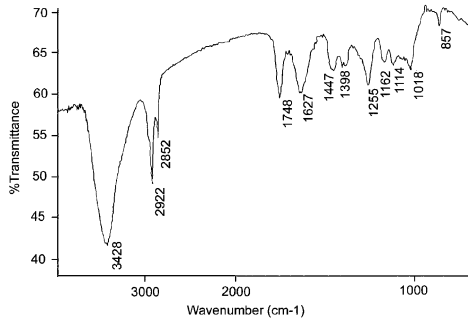

Figure 5. IR spectrum of helical nanofibers.

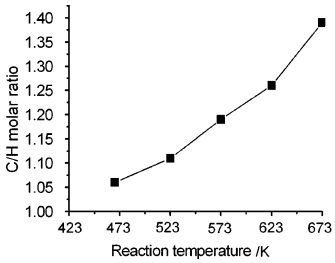

Figure 6. C/H molar ratio changes of the nanofibers with the reaction temperature.

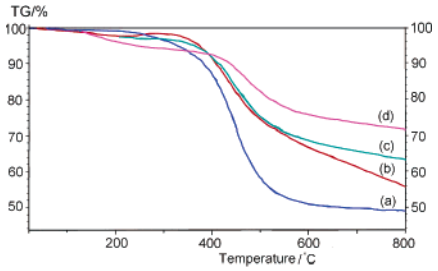

Figure 7. TG analysis of the nanofibers prepared at different temperatures: (a) 468 K, (b) 523 K, (c) 573 K, and (d) 673 K.

helical senses, simultaneously resulting in helical reversals, as shown in Figure 3B−D, indicated by arrows. TEM images indicate that the catalyst particles included at the nodes of the twin helices usually show regular, faceted rhombic shapes (Figure 3E). The majority of the angles between the two twin helices are about 70° or 110°.

The XRD pattern of the helical nanofibers is shown in Figure 4. In the range below 40°, there is a broad diffraction peak in high intensity. No diffraction peak of graphitic carbon appears, revealing an amorphous feature of the helical nanofibers. In the diffraction range over 40°, the typical diffraction peaks of metallic copper can be clearly observed. No diffraction peaks of other metallic impurity are determined. Energy-dispersive X-ray (EDX) analysis does not reveal any other metal impurity, especially Ni, Co, or Fe, as well. These investigations confirm that no effect of added impurity is involved in the nanofiber growth. Therefore, in this study, copper nanocrystals are indeed responsible for the growth of these helical nanofibers.

Raman measurement shows that the nanofibers do not show any prominent peak except for the background emission ranging from 1000 to 1800 cm^{-1}, suggesting the formation of a polymer-like structure. In other words, the nanofibers have a high bonded hydrogen content.

Figure 5 shows the infrared (IR) spectrum of the helical nanofibers. The absorption peaks at 3428 cm^{-1} and 1748 cm^{-1} are ascribed to the stretching vibrations of −O−H and −C═O, respectively, indicating the slight oxidation of the product or presence of adsorbed water (after being taken out from the reactor). These peaks at 2922 cm^{-1}, 2852 cm^{-1}, and 1447 cm^{-1} can be ascribed to the −C−H vibration in $-CH_2$ or −CH. The peak at 1627 cm^{-1} can be assigned to the −C═C− stretching vibration. The −C−H deformation in $-CH_3$ induces the peak at 1398 cm^{-1}. It must be noted that there is an obvious absorption peak at 1018 cm^{-1}, which is near the typical IR absorption peak at 1014 cm^{-1} of *trans*-polyacetylene.[3] On the basis of the IR feature, we know the nanofibers consist of both unsaturated −CH═CH− and saturated −CH, $-CH_2$, and $-CH_3$ groups. Possibly, the conjugate action of carbon−carbon double bonds contributes to the weak *trans*-polyacetylene feature. The IR spectrum further confirms the high hydrogen content in the nanofibers. In the IR spectra of the nanofibers prepared at higher temperature (523−673 K), there are no peaks near 1014 cm^{-1}, indicating the thorough disappearance of the *trans*-polyacetylene feature. In addition, IR analysis suggests that the liquid products condensed at both ends of the reactor are oligomers of complex composition.

It can be determined by an elemental analyzer (Flash EA1112) that the C/H molar ratio of the nanofibers prepared at 468 K is 1.06:1 (Figure 6). In comparison with the IR and Raman analysis, the C/H molar ratio quantitatively indicates the high hydrogen content of the nanofibers. C/H molar ratios of the helical nanofibers prepared at elevated reaction temperatures are as follows: 1.11 at 523 K, 1.19 at 573 K, 1.26 at 623 K, and 1.39 at 673 K.[36] It is apparent that the hydrogen content of the products decreases enormously with the increase of reaction temperature.

Thermogravimetric (TG) analysis (Figure 7) has been used to determine the thermal stability of the products. When the nanofibers are heated, they undergo thermal decomposition to release new (gaseous) hydrocarbon species with a low molecular weight, resulting in a weight loss of the nanofibers. Comparing the weight loss curves of several products prepared at different temperatures, we observe that the weight loss and the weight loss rate reduce with the increase of the reaction temperature. Obviously, the thermal stability of the nanofibers increases with the reaction temperature. As for the nanofibers prepared at 468 K, they undergo a rapid weight loss before they are heated to 873 K and lose half their weight when heated to 1073 K.

4. Discussion

Microstructure of the Helical Nanofibers. Our experimental results show that the interaction of copper nanocrystals with acetylene can produce regularly coiled nanofibers at the low temperature of 468 K, in contrast to previous reports that pure metallic copper shows no activity for the carbon deposition of hydrocarbon. The nanofibers are not graphitic as shown by XRD analysis. High-resolution transmission electron microscope (HRTEM) images clearly exhibit the amorphous structure of the nanofibers.[38] IR and Raman analyses reveal that they contain a high content of hydrogen. The C/H molar ratio quantitatively confirms the high hydrogen content. About 6% hydrogen is

released from the acetylene precursor during the nanofiber growth. On the basis of the XRD, IR, Raman, and C/H ratio analyses we conclude that the nanofibers exhibit a polymer-like structure. It is a new type of nanofiber obtained from hydrocarbon interaction with metal catalyst via heterogeneous catalysis. Their structures are entirely different from the carbon nanofibers prepared by carbon deposition of acetylene on Ni, Co, Fe, and so forth nanoparticles at high temperature. Therefore, it can be concluded that the general vapor−liquid−solid mechanism or the dissolution−diffusion−precipitation mechanism based on the bulk diffusion of carbon through the catalyst particles are not suitable for the nanofiber growth in our study. It can be speculated that the deposition reaction of acetylene over copper nanocrystal surfaces at 468 K is carried out by both coupling (94%) and decomposition (6%) of acetylene molecules associated with the nanofiber formation.

While the helical nanofibers form mainly via a catalytic coupling (or polymerization) process, the IR spectrum of the nanofibers is clearly different from Shirakawa-type polyacetylene.[3] Moreover, the decomposition of a small fraction of acetylene leads to a higher carbon content of the nanofibers than hydrogen. Therefore, the reaction is substantially different from the general polymerization reaction of acetylene in homogeneous catalysis. The helical nanofibers, synthesized by chemical vapor deposition using acetylene as the gas source and copper nanoparticles as a catalyst at 468 K, should not be referred to as polyacetylene nanofibers. It is more suitable to classify them as a new type of amorphous carbon nanofiber, which is a mixture of solid polymers from acetylene coupling and carbon from acetylene decomposition.

Reaction Mechanism. As mentioned in the Introduction, the interaction of acetylene with copper surfaces under UHV conditions results in reversible desorption of adsorbed acetylene and also rich surface reaction products.

(1) Benzene is the main product, which forms over all three low-index planes.[23,24,26,27] In addition, ethylene, butadiene, and cyclooctatetraene form on Cu(111).[27]

(2) Slight carbon deposition occurs on Cu(110) and (001).[23,24,26] It also occurs on Cu(111) although in a small amount undetectable by C 1s XPS.[27]

(3) New hydrocarbon species with good stability form on Cu(110) and (001), which can survive the thermal desorption process up to a higher temperature.[24−26] Kyriakou et al. observed the extensive deposition of hydrocarbon species on Cu(111) at atmospheric pressure, although they did not report the formation of new hydrocarbon species on Cu(111) under UHV conditions.[27]

From the above results, we can infer that it is possible to prepare carbon or hydrocarbon (or their mixture) nanofibers using Cu nanocatalysts in the same temperature region at normal pressure of acetylene without any additive such as hydrogen, if the reaction follows well the surface reaction of acetylene on Cu single-crystal surfaces under UHV conditions. Our experimental results demonstrate that helical nanofibers can be synthesized using copper nanocrystals as a catalyst at the lowest temperature of 468 K under normal pressure of pure acetylene. Obviously, the reaction temperature is in the same region as applied under UHV conditions. The copper nanoparticles should be exposed mainly with (111), (110), and (001) low-index surfaces.[38] Coincidentally, the nanofibers are a polymer-like mixture of hydrocarbon (polymers from acetylene coupling) and a small amount of carbon. Heat treatment will induce the evolution of new, small hydrocarbon molecules because of the C−H cleavage and structural reconfiguration of the nanofibers and the ensuing weight loss. They can survive the heat treatment process up to about 900 K, which seems very consistent with the EEL spectrum analysis reported by Avery.[24] In addition, a small amount of liquid oligomers form and then condense at both ends of the reactor. IR analysis shows a complex spectrum from a mixture of extensive oligomers, in agreement with the mass spectrum analysis reported by Kyriakou et al.[27] The simultaneous formation of carbon, liquid oligomers, and solid polymers in our study agrees well with these formed under UHV conditions. Therefore, the reaction with copper nanocatalysts at an atmospheric pressure of pure acetylene at 468 K does mimic the surface reactions on copper single-crystal surfaces under UHV conditions.

Combining the available results obtained using copper single crystals under UHV conditions with our results obtained using a copper nanocatalyst at atmospheric pressure, we can basically formulate the main reaction process of acetylene on copper nanocrystal surfaces in our study as follows:

$$C_2H_2(g) \rightarrow C_2H_2(a)$$

$$\text{Benzene} \quad C_2H_2(a) + C_2H_2(a) \rightarrow C_4H_4(a) \tag{1}$$

$$C_4H_4(a) + C_2H_2(a) \rightarrow C_6H_6(a) \tag{2}$$

$$\text{Cyclooctatetraene} \quad C_4H_4(a) + C_4H_4(a) \rightarrow C_8H_8(a) \tag{3}$$

Other liquid oligomers

$$mC_2H_2(a) \rightarrow -(CH{=}CH)_m- \ (m > 4) \tag{4}$$

$$\text{Solid polymers} \quad nC_2H_2(a) \rightarrow -(CH{=}CH)_n- \ (n > m) \tag{5}$$

$$\text{Carbon} \quad C_2H_2(a) \rightarrow C_2(a) + 2H(a) \tag{6}$$

$$2H(a) \rightarrow H_2(g) \tag{7}$$

$$\text{Ethylene} \quad C_2H_2(a) + 2H(a) \rightarrow C_2H_4(a) \tag{8}$$

$$\text{Butadiene} \quad C_4H_4(a) + 2H(a) \rightarrow C_4H_6(a) \tag{9}$$

Liquid oligomer or solid polymer hydrogenation:

$$-(CH{=}CH)_n- + H(a) \rightarrow -(CH{=}CH)_{n-1}CH{=}CH_2 \tag{10}$$

$$-(CH{=}CH)_{n-1}CH_2CH_3, \ (3H(a)) \tag{11}$$

or

$$-(CH{=}CH)_xCH_2CH_2(CH{=}CH)_y- \ (2H(a), \ x + y + 1 = n) \tag{12}$$

The benzene formation proceeds by the association of two adsorbed acetylene molecules to form a C_4H_4 metallocycle intermediate (reaction 1), which then reacts with a third acetylene molecule (reaction 2). This has been confirmed by extensive studies. A pericyclic mechanism involving dimerization of two C_4H_4 intermediate is proposed by Kyriakou et al. to account for the formation of cyclooctatetraene (reaction 3).[27] Some adsorbed acetylene molecules will couple to form liquid oligomers (reaction 4), which subsequently desorb (or vaporize) from the catalyst particle surfaces at the reaction temperature and finally condense at the two ends of the reactor. Solid polymers form when a large number of acetylene molecules are involved in a coupling or polymerization process (reaction 5).

The C−H cleavage will lead to irreversible carbon deposition (reaction 6) in a small amount as revealed by the C/H molar ratio analysis, because there is no added hydrogen to inhibit the carbon deposition in this study. The C−H cleavage process also produces atomic hydrogen in an adsorbed state, but the H_2 formation (reaction 7) is impossible, since no added hydrogen is coadsorbed with acetylene.[23] This is reasonable in that the H(a) with a high activity competes to react with adsorbed acetylene molecules, C_4H_4 intermediates, and other transition state intermediates for benzene, cyclooctatetraene, liquid oligomer, and solid polymer formation. It will react with acetylene to produce ethylene (reaction 8) and with C_4H_4 intermediate to butadiene (reaction 9), respectively.[27] From the 1.06:1 C/H molar ratio of the nanofibers, about 6% of the adsorbed acetylene molecules that contribute to the nanofiber growth encounter decomposition (reaction 6), and the corresponding 6% hydrogen are released by the formation of ethylene (reaction 8) and butadiene (reaction 9), and so forth, and by liquid oligomer hydrogenation (reactions 10−12). In fact, there must be some hydrogen released from the C−H cleavage with the solid polymers (reactions 10−12).

The hydrogenation of the transition state intermediates of liquid oligomers and solid polymers will cause their growth termination and reduce their molecular chain lengths or molecular weights (reaction 10). In addition, hydrogenation will also add hydrogen in the molecular chain, resulting in the presence of $-CH_2$ (reactions 11 and 12) and $-CH_3$ (reaction 11) groups. This accounts for the IR analysis result that the nanofibers contain saturated $-CH_2$ and $-CH_3$ groups. Most important of all, these hydrogenation reactions considerably decrease the chain length of conjugated carbon−carbon double bonds owing to the introduction of saturated groups or the reduction of the whole molecular chain length. For example, for a polymer with 100 C atoms with conjugated double bonds, the addition of 2H(a) will reduce the conjugated chain length to 50 carbon atoms and of 6H(a) to 25 on the average, respectively (reaction 12). Shirakawa et al. reported the structural changes of polyacetylene with the reaction temperature.[3] The product prepared at 195 K was *cis*-polyacetylene with a marked IR peak at 741 cm^{-1}. The resultant product at 293 K contained both *cis*- and *trans*-polyacetylene structures. However, when the reaction temperature was increased to 423 K, the product showed an entire *trans*-polyacetylene structure with a prominent IR peak at 1014 cm^{-1}. According to the structural changes with reaction temperature, we can speculate that the nanofibers prepared at 468 K should exhibit a *trans*-polyacetylene structure on the condition that the nanofibers contain only solid polymers from acetylene coupling and undergo no hydrogenation. Our IR analysis indicates that the molecular structures of the nanofibers are apparently different from Shirakawa-type *trans*-polyacetylene, although the reaction proceeds mainly via acetylene coupling. It merely shows a weak IR peak at 1018 cm^{-1}, near 1014 cm^{-1} of *trans*-polyacetylene. Therefore, it can be known that the addition of hydrogen from the C−H cleavage indeed seriously shortens the chain length of conjugated carbon−carbon double bonds of the solid polymers. Possibly, the mixture of carbon from the C−H cleavage with the solid polymers also weakens the *trans*-polyacetylene feature of the nanofibers.

Recent significant progress in both theoretical and experimental fields leads to the rich detail of the interaction of molecules with metal surfaces. The adsorption properties, possible surface intermediates, and possible evolution products of acetylene on different crystal faces can be studied using various calculation methods and STM investigations.[17−19,28−33,39−41] Yuan et al. reported a first-principles study of acetylene and its evolution products (CCH, C_2, and CCH_2) on the Cu(001) surface using the density functional method with cluster models.[29] The results agree well with the available experimental results. CCH_2 is found to be more stable than C_2H_2 on Cu(001). Therefore, it is possible that the insertion (or addition) of these thermal evolution products (in particular, CCH_2) into the molecular chains of the solid polymers will also reduce the chain length of the conjugated carbon−carbon double bonds, resulting in further weakness of the *trans*-polyacetylene feature.

The catalytic measurements reported by Kyriakou et al. indicate that a much higher yield of butadiene and high molecular weight oligomers form at atmospheric pressure in the case of a 10:1 hydrogen/acetylene mixture. The added hydrogen indeed enormously promotes the hydrogenation reaction. This will inevitably reduce solid polymer yields by promoting chain termination and increase oligomer yields, some of which cannot vaporize from the copper catalyst surfaces even at the reaction temperature of 523 K. As a result, these oligomers will block the copper nanoparticle surfaces, resulting in a rapid catalyst deactivation. In our study, pure acetylene without added hydrogen at atmospheric pressure is favorable for the formation of solid polymers; hence, nanofibers can be obtained.

IR analysis of the nanofibers prepared at elevated temperatures (523−673 K) shows no peaks at (or near) 1014 cm^{-1}. C/H molar ratio analysis shows their carbon contents increase with reaction temperature. It is reasonable that the C−H cleavage increases at higher temperature and promotes the carbon deposition. The nanofibers form mainly via a thermal decomposition mechanism of acetylene at higher temperature. Higher carbon contents effectively improve their thermal stability and then inhibit the weight loss during heat treatment or TG analysis (Figure 7). The hydrogen produced from enhanced C−H cleavage escapes by the formation of more ethylene, butadiene, and liquid oligomers and also reacts with solid polymers. Enhanced hydrogenation to solid polymers further shortens the chain length of conjugated carbon−carbon double bonds. The higher carbon contents and less-conjugated chain lengths of the solid polymers account for the lack of any *trans*-polyacetylene feature of the nanofibers prepared at higher temperature.

On the basis of the change trend of the C/H molar ratios (Figure 6) with the decrease of reaction temperature, it can be inferred that helical nanofibers approximately with a 1:1 C/H molar ratio can be synthesized, if copper nanocrystals can catalyze acetylene coupling to form nanofibers at about 423 K, the temperature at which Shirakawa et al. synthesized *trans*-polyacetylene. At this temperature, carbon deposition from the C−H cleavage reduces and solid polymer hydrogenation decreases effectively. The nanofibers will contain a higher purity of solid polymers with an increased conjugated chain length and, hence, exhibit a promoted *trans*-polyacetylene feature. However, our experimental results reveal that the lowest temperature for nanofiber growth is 468 K. In fact, from the previous results, we know that the new hydrocarbon species (or solid polymers) can form below 420 K.[23−26] Therefore, it can be inferred that the lowest starting temperature of 468 K is necessary to provide enough driving force for the "extrusion" of solid polymers from the copper nanocrystal surfaces to form nanofibers. We have tried several other metal nanoparticles such as Ni, Co, or Fe under the same reaction conditions. However, their triggering temperatures for nanofiber growth are over 623

K**,** consistent with the literature.[42] These reactions only lead to carbon nanofibers. As for Ni, this reaction channel is in good agreement with the result revealed under UHV conditions in which acetylene is completely dehydrogenated near 300 K on nickel surfaces.[21,22] This implies that only carbon nanofibers can be obtained at atmospheric pressure. Regarding copper alloy catalysts (50% w/w), addition of Ni, Co, or Fe leads to elevated triggering temperature over 513 K. Therefore, further efforts to seek suitable metal catalysts (or alloys) and modified reaction conditions are necessary to further lower the reaction temperature.

We have also tried ethylene as a gas source. However, no reactions take place from room temperature to 773 K with other conditions unchanged. This is consistent with the previous results under UHV conditions, e.g., when adsorbed on a Cu(110) surface, ethylene itself desorbs at 210 K with no evidence of reaction.[23] This further confirms that the reaction mechanism under UHV conditions does reflect the reaction mechanism under practical conditions at atmospheric pressure. In comparison with ethylene, acetylene shows the excellent richness of its catalytic chemistry on copper surfaces.

A few researchers reported the carbon deposition of acetylene at medium temperature (not enhanced by microwave, radio frequency plasma, etc.). Baker reported the carbonaceous deposits from the platinum−iron catalyzed decomposition of acetylene at 673 K.[43] Synder et al. synthesize carbon fibers with Fe-based catalyst at 673 K.[44] Motojima et al. reported the carbon deposition of acetylene with Ni catalyst over 623 K.[42] Although there are reports on the synthesis of carbon nanofibers or nanotubes by plasma-enhanced chemical vapor deposition at low temperature, even at room temperature,[45,46] we believe this is the lowest temperature (468 K) for general metal-catalyzed chemical vapor deposition of hydrocarbon for (amorphous) carbon nanofiber growth.

5. Conclusions

We have synthesized amorphous helical carbon nanofibers at low temperature using copper nanocrystals as a catalyst and acetylene as a gas source at normal pressure. These nanocoils exhibit a symmetric growth mode in the form of twin helices. IR, XRD, Raman, and C/H molar ratio reveal they have a polymer-like structure with a weak *trans*-polyacetylene feature. They should be a mixture of solid polymers from acetylene coupling and a small amount of carbon from acetylene decomposition.

On the basis of the extensive studies of acetylene adsorption, desorption properties, and surface reactions on copper surfaces under UHV conditions, along with our studies at atmospheric pressure, a reaction mechanism has been proposed. Under the chosen conditions, acetylene couples to form gaseous products, liquid oligomers, and solid polymers, and also slightly decomposes to produce a small amount of carbon. The addition of hydrogen from the C−H cleavage and the insertion of the thermal evolution products (CCH_2, CCH, and C_2) of adsorbed acetylene to the solid polymer intermediates lead to the weak *trans*-polyacetylene feature of the nanofibers. Additionally, the mixture of carbon with the solid polymers also weakens the polyacetylene feature. The reactions under practical conditions indeed mimic the reaction mechanism revealed under UHV conditions. Acetylene shows excellent richness of its catalytic chemistry on copper surfaces. In comparison with previous publications that reported the prominent formation of benzene and others, our study presents the nanofiber growth and provides an excellent example for the synthesis of new types of nanofibers based on these studies under UHV conditions. This is the lowest temperature to synthesize amorphous helical carbon nanofibers by ordinary metal-catalyzed thermal chemical vapor deposition of hydrocarbon.

References and Notes

(1) Ito, T.; Shirakawa, H.; Ikeda, S. *J. Polym. Sci., Part A: Polym. Chem.* **1974**, *12*, 11.
(2) Hall, N. *Chem. Commun.* **2003**, 1.
(3) Shirakawa, H.; Ikeda, S. *Polym. J.* **1971**, *2*, 231.
(4) Amelinckx, S.; Zhang, X. B.; Bernaerts, D.; Zhang, X. F.; Ivanov, V.; Nagy, J. B. *Science* **1994**, *265*, 635.
(5) Baker, R. T. K.; Harris, P. S.; Thomas, R. B.; Waite, R. J. *J. Catal.* **1973**, *30*, 86.
(6) Motojima, S.; Itoh, Y.; Asakura, S.; Iwanaga, H. *J. Mater. Sci.* **1995**, *30*, 5049.
(7) Perez-Cabero, M.; Rodriguez-Ramos, I.; Guerrero-Ruiz, A. *J. Catal.* **2003**, *215*, 305.
(8) Baker, R. T. K. *Carbon* **1989**, *27*, 315.
(9) Yang, R. T.; Chen, J. P. *J. Catal.* **1989**, *115*, 52.
(10) Alstrup, I. *J. Catal.* **1988**, *109*, 241.
(11) Jong, K. P. D.; Geus, J. W. *Catal. Rev. Sci. Eng.* **2000**, *42*, 481.
(12) Tavares, M. T.; Bernardo, C. A.; Alstrup, I.; Rostrupnielsen, J. R. *J. Catal.* **1986**, *100*, 545.
(13) Bernardo, C. A.; Alstrup, I.; Rostrupnielsen, J. R. *J. Catal.* **1985**, *96*, 517.
(14) Nishiyama, Y.; Tamai, Y. *J. Catal.* **1976**, *45*, 1.
(15) Lambert, R. M.; Omerod, R. M. In *Surface Reactions*; Springer Series in Surface Science; Madix, R. J., Ed.; Springer-Verlag: Berlin, 1994; Vol. 34, Chapter 4.
(16) Sheppard, N. *Annu. Rev. Phys. Chem.* **1988**, *39*, 589.
(17) Dunphy, J. C.; Rose, M.; Behler, S.; Ogletree, D. F.; Salmeron, M.; Sautet, P. *Phys. Rev. B* **1998**, *57*, R12705.
(18) Stipe, B. C.; Rezaei, M. A.; Ho, W. *Science* **1998**, *280*, 1732.
(19) Stipe, B. C.; Rezaei, M. A.; Ho, W. *Phys. Rev. Lett.* **1998**, *81*, 1263.
(20) Szanyi, J.; Paffett, M. T. *J. Am. Chem. Soc.* **1995**, *117*, 1034.
(21) Demuth, J. E. *Surf. Sci.* **1980**, *93*, 127.
(22) Fischer, T. E.; Kelemen, S. R. *Surf. Sci.*, **1978**, *74*, 47.
(23) Outka, D. A.; Friend, C. M.; Jorgensen, S.; Madix, R. J. *J. Am. Chem. Soc.* **1983**, *105*, 3468.
(24) Avery, N. R. *J. Am. Chem. Soc.* **1985**, *107*, 6711.
(25) Marinova, T. S.; Stefanov, P. K. *Surf. Sci.* **1987**, *191*, 66.
(26) Dvorak, J.; Hrbek, J. *J. Phys. Chem. B* **1998**, *102*, 9443.
(27) Kyriakou, G.; Kim, J.; Tikhov, M. S.; Macleod, N.; Lambert, R. M. *J. Phys. Chem. B* **2005**, *109*, 10952.
(28) Hasegawa, K.; Dino, W. A.; Kasai, H.; Okiji, A. *Surf. Sci.* **2000**, *454*−*456*, 1052.
(29) Yuan, L. F.; Yang, J. L.; Li, Q. X.; Zhu, Q. S. *J. Chem. Phys.* **2002**, *116*, 3104.
(30) Olsson, F. E.; Persson, M.; Lorente, N.; Lauhon, L. J.; Ho, W. *J. Phys. Chem. B* **2002**, *106*, 8161.
(31) Bernardo, C. G. P. M.; Gomes, J. A. N. F. *J. Mol. Struct.* **2003**, *629*, 251.
(32) Ostrom, H.; Nordlund, D.; Ogasawara, H.; Weiss, K.; Triguero, L.; Pettersson, L. G. M.; Nilsson, A. *Surf. Sci.* **2004**, *565*, 206.
(33) Mingo, N.; Makoshi, K. *Phys. Rev. Lett.* **2000**, *84*, 3694.
(34) Weinelt, M.; Huber, W.; Zebisch, P.; Steinruck, H. P.; Ulbricht, P.; Birken-heuer, U.; Boettger, J. C.; Rosch, N. *J. Chem. Phys.* **1995**, *102*, 9709.
(35) Mingo, N.; Makoshi, K. *Appl. Surf. Sci.* **2000**, *162*, 227.
(36) Qin, Y.; Zhang, Z. K.; Cui, Z. L. *Carbon* **2003**, *41*, 3072.
(37) Qin, Y.; Li, H.; Zhang, Z. K.; Cui, Z. L. *Org. Lett.* **2002**, *4*, 3123; **2005**, *7*, 523 (erratum).
(38) Qin, Y.; Zhang, Z. K.; Cui, Z. L. *Carbon* **2004**, *42*, 1917.
(39) Hu, X. F.; Chen, C. J.; Tang, J. C. *Surf. Sci.* **1996**, *365*, 319.
(40) Triguero, L.; Petterson, L. G. M.; Minaev, B.; Agren, H. *J. Chem. Phys.* **1998**, *108*, 1193.
(41) Lorente, N.; Persson, M. *Phys. Rev. Lett.* **2000**, *85*, 2997.
(42) Motojima, S.; Kawaguchi, M.; Nozaki, K.; Iwanaga, H. *Appl. Phys. Lett.* **1990**, *56*, 321.
(43) Baker, R. T. K.; Waite, R. J. *J. Catal.* **1975**, *37*, 101.
(44) Snyder, C. S.; Mandeville, W. H.; Tennent, H. G.; Truesdale, L. K.; Barber, J. J. WO Pat. Appl. 89/07163, 1989.
(45) Boskovic, B. O.; Stolojan, V.; Khan, R. U. A.; Haq, S.; Silva, S. P. *Nat. Mater.* **2002**, *1*, 165.
(46) Hofmann, S.; Ducati, C.; Robertson, J.; Kleinsorge, B. *Appl. Phys. Lett.* **2003**, *83*, 135.